

Multifactor Change in Western U.S. Nighttime Fire Weather

ANDREW M. CHIODI,^{a,b} BRIAN E. POTTER,^c NARASIMHAN K. LARKIN,^c AND D. E. HARRISON^b

^a Cooperative Institute for Climate, Ocean and Ecosystem Studies, University of Washington, Seattle, Washington

^b NOAA/Pacific Marine Environmental Laboratory, Seattle, Washington

^c Pacific Wildland Fire Sciences Laboratory, USDA Forest Service, Seattle, Washington

(Manuscript received 17 September 2024, in final form 6 January 2025, accepted 22 January 2025)

ABSTRACT: Reports from western U.S. firefighters that nighttime fire activity has been increasing during the spans of many of their careers have recently been confirmed by satellite measurements over the 2003–20 period. The hypothesis that increasing nighttime fire activity has been caused by increased nighttime vapor pressure deficit (VPD) is consistent with recent documentation of positive, 40-yr trends in nighttime VPD over the western United States. However, other meteorological conditions such as near-surface wind speed and planetary boundary layer depth also impact fire behavior and exhibit strong diurnal changes that should be expected to help quell nighttime fire activity. This study investigates the extent to which each of these factors has been changing over recent decades and, thereby, may have contributed to the perceived changes in nighttime fire activity. Results quantify the extent to which the summer nighttime distributions of equilibrium dead woody fuel moisture content, planetary boundary layer height, and near-surface wind speed have changed over the western United States based on hourly ERA5 data, considering changes between the most recent decade and the 1980s and 1990s, when many present firefighters began their careers. Changes in the likelihood of experiencing nighttime meteorological conditions in the recent period that would have registered as unusually conducive to fire previously are evaluated considering each variable on its own and in conjunction (simultaneously) with one another. The main objective of this work is to inform further study of the reasons for the observed increases in nighttime fire activity.

SIGNIFICANCE STATEMENT: Western U.S. firefighters have reported a problematic rise in nocturnal wildfire activity. Verifying their hypothesis that meteorological variability is responsible is a first step toward better understanding the predictability of the underlying processes. This study expands upon our previous investigation of multidecadal change in seasonally averaged nocturnal vapor pressure deficit by looking at changes in the frequency of dry-fuel nights over the western United States and their coincidence with other fire-conducive nocturnal meteorological conditions. Dry-fuel nights have become >10× more frequent in the 2010s compared to the 1980s and 1990s in some regions. Over 81% of the study area, increasing dry-fuel night frequency has been compounded by the double, or triple, threats of simultaneously windier and deeper planetary boundary layers.

KEYWORDS: Forest fires; Humidity; Boundary layer; Wind effects; Atmosphere-land interaction; Diurnal effects


1. Introduction

Fighting wildfires requires meticulous planning, and a key element in that depends on the diurnal cycle. Crews cannot safely engage fire in the dark, except in special circumstances. They wake before dawn so that they can start their work early in the day, when the fire is relatively calm. Wildfire behavior, characterized by metrics such as spread rate, intensity, and flame length (Archibald et al. 2013), typically increases throughout the day, into early evening or possibly sunset. This means that firefighters need to be most cautious toward the end of their shift when they are also most fatigued. Nighttime is a crucial period for them to rest, both physically and mentally. Fortunately, fire behavior typically diminishes, or “lays down,” at sunset and stays relatively calm through the night, allowing them this rest. Calmer nocturnal fire behavior is anecdotally tied to “nighttime humidity recovery,” when relative humidity rises and brings fuel moisture with it.

Over the last decade, fire managers have expressed concern that fires are not laying down at night as much as they used to (Little 2020). Fires that maintain daytime characteristics into the evening and smaller nocturnal increases in relative humidity are their main concerns. They largely attribute this to lack of humidity recovery, speculating that the timing and magnitude of humidity recovery have changed over the years in ways that hamper firefighting efforts.

U.S. firefighters’ perceptions of increasing nighttime fire activity have recently been confirmed by Freeborn et al. (2022) who found that the sum of fire radiative power (FRP; Freeborn et al. 2014) detected by the Aqua and Terra Moderate Resolution Imaging Spectroradiometers (MODIS; Giglio et al. 2006, 2016) over the conterminous United States at night has increased by approximately one-half (+54%) between the later and first half of their 2003–20 study period. Freeborn et al. (2022) also examined the probability of nighttime persistence (daytime followed by nighttime MODIS fire detects) and found it to be mainly characteristic of larger (>20 km²) wildfires burning amid low-percentile 1000-h dead fuel moisture conditions (Jolly et al. 2019; Abatzoglou and Williams 2016), but fuel moisture trends were not examined.

Vapor pressure deficit (VPD) is dependent on atmospheric temperature and moisture content and determines the rate at

 Denotes content that is immediately available upon publication as open access.

Corresponding author: Andrew M. Chiodi, andy.chiodi@noaa.gov

DOI: 10.1175/JCLI-D-24-0473.1

© 2025 American Meteorological Society. This published article is licensed under the terms of the default AMS reuse license. For information regarding reuse of this content and general copyright information, consult the AMS Copyright Policy (www.ametsoc.org/PUBSReuseLicenses).

Brought to you by NOAA Seattle Library | Unauthenticated | Downloaded 05/09/25 11:17 PM UTC

which woody fuels lose moisture to the air. VPD affects fire behavior through its influence on fuel moisture. Monthly to seasonal and regionally averaged VPD have been found to correlate with the annual burned area over several western U.S. regions (Seager et al. 2015), including the interior Southwest (Williams et al. 2014; Mueller et al. 2020) and California (Williams et al. 2019; Jacobson et al. 2022).

Chiodi et al. (2021) explored nighttime VPD change using seasonal averages calculated from the fifth major global reanalysis produced by the European Centre for Medium-Range Forecasts (ERA5; Hersbach et al. 2020). They showed that the anecdotal concerns are indeed supported by observational evidence of positive trends in nighttime VPD over the western United States during the last 40 years. Balch et al. (2022) extended this line of inquiry globally, identifying the areas around Earth where, based on their linear statistical model of the VPD–fire relationship, nighttime VPD has risen above thresholds estimated to be low enough to calm fire activity at night.

While fuel moisture may increase overnight—and observations clearly show this (e.g., Weise et al. 2005)—rising relative humidity is only one of several changes in the nocturnal atmosphere that drive fire behavior. The cessation of solar heating at the ground also decreases surface turbulence and allows the formation of the nocturnal stable layer (Stull 1988). This stable layer is the nighttime manifestation of the planetary boundary layer (PBL), the region of Earth’s atmosphere modified directly by surface fluxes. The height of the PBL depends on the balance between thermodynamic stability and wind shear. At night, increasing stability results in lower mean winds and less turbulence in the PBL and subsequently more moderate fire spread and intensity. The cooling at the ground combined with any upward moisture flux from the soil produces higher humidity. Cooling also traps smoke at the ground, which can further subdue fire behavior.

Wind affects fire behavior by providing convective heat transport to preheat and dry fuels ahead of the combustion front and, by tilting the flames, increases the radiative flux to the fuels ahead of the fire. In combination with terrain slope (Nelson 2002), wind plays a key role in determining the rate of spread of a wildfire (cf. Cruz et al. 2020) and is one of the fundamental meteorological inputs into fire behavior models (Rothermel 1972; Andrews et al. 2005) and fire danger rating systems (Jolly et al. 2024) that are used over the western United States and in other fire-prone regions.

Dead woody fuel equilibrium moisture content (EMC) is a proxy for the moisture content of dead fine fuels, which consist of dead vegetation less than approximately 6 mm (0.25 in.). Fine fuels dry rapidly as EMC decreases, absent direct contact with water (*e*-folding time scales < 1 h). Fine fuels have a large surface area-to-volume ratio, allowing them to burn readily when dry and, when present and dry, play an important role in driving fire spread rates (Rothermel 1972). Like VPD, EMC can be estimated from atmospheric temperature and moisture content. EMC is highly correlated with VPD but distributed differently. Owing to our interest in investigating the extent to which smaller nocturnal humidity increases have led to drier fuels at night, we examine how the nocturnal distribution of fire-conductive EMC extremes has changed between an earlier

period and the most recent decade (2011–20) when nighttime wildfire activity has increased. Following the approach used by Chiodi et al. (2021), the earlier period is defined as 1981–2000, representing the early career years of many current firefighters, when they formed their concepts of historically normal wildfire behavior.

It is reasonable to expect long-term changes in nocturnal PBL height, wind speed, and EMC to all drive changes in nighttime fire activity. We are therefore interested in better understanding the extent to which these nocturnal weather factors have changed over recent decades. We evaluate this question using hourly resolution wind speed at 10 m above ground level (u_{10} ; m s^{-1}), PBL height (H_{PBL} ; m), and dead woody fuel EMC (percent dry fuel weight), all derived from ERA5 data over western U.S. summer nights. Our analysis is designed to address two main objectives: One is improving our understanding of where and by how much the frequency of nocturnal u_{10} , H_{PBL} , and EMC fire-conductive extremes has risen in the recent period compared to earlier decades. The complementary objective is understanding where the simultaneous occurrence of such conditions—two or more variables reaching fire-conductive extremes at the same time—has increased.

2. Data and methods

Hourly values of air temperature and dewpoint temperature at 2-m height above ground, u_{10} , and H_{PBL} were obtained from ERA5 at 25-km horizontal resolution.

In ERA5, H_{PBL} is determined using a bulk Richardson number approach. This is based on work by Seidel et al. (2012) that found the bulk Richardson approach performed best for determining H_{PBL} from model as well as radiosonde profiles. The bulk Richardson number can be expressed as

$$\text{Ri}_b(z) = \frac{gz}{\theta_{\text{vsfc}}} \frac{[\theta_v(z) - \theta_{\text{vsfc}}]}{u(z)^2}, \quad (1)$$

where g is the gravitational acceleration (m s^{-2}), z is the depth of a layer with the base at the ground (m), θ_{vsfc} is the virtual potential temperature at the ground (K), $\theta_v(z)$ is the virtual potential temperature at height z (K), and $u(z)$ is the horizontal wind speed at height z (m s^{-1}). The $\text{Ri}_b(z)$ is zero at $z = 0$, and the PBL height is defined in this method as the lowest height where $\text{Ri}_b(z) = 1/4$. Subsequently, one can set Eq. (1) equal to $1/4$ and solve for H_{PBL} :

$$H_{\text{PBL}} = \frac{u_{\text{PBL}}^2 \theta_{\text{vsfc}}}{4g[\theta_v(H_{\text{PBL}}) - \theta_{\text{vsfc}}]}. \quad (2)$$

The wind speed term u_{PBL}^2 represents the wind shear between Earth’s surface and H_{PBL} , with the former assumed to be zero. The potential temperature difference in the denominator is a measure of thermodynamic stability. Greater surface stability results in a shallower PBL, a point key to our later discussions.

The EMC of woody fuel is the weight of water in the fuel as a percentage of the dry weight of fuel at the point that the transport of moisture from the fuel to the atmosphere equals that from the atmosphere to the fuel. EMC is a proxy for

“fine” or 1-h dead fuel moisture,¹ in the absence of precipitation or other sources of direct contact between the fuels and liquid water. In later sections, we use the phrase “dry fuel” to refer to low EMC values for brevity, recognizing that precipitation may make this imprecise. EMC was calculated from ERA5 data by first calculating relative humidity (RH) at 2-m height based on the ratio of the actual partial pressure of water vapor in air e_a to the thermodynamic equilibrium pressure (a.k.a. “saturation” pressure) of water vapor over a plane surface of water e_s :

$$\text{RH} = 100 \times \frac{e_a}{e_s},$$

with e_s and e_a calculated from 2-m temperature T_c and dewpoint temperature T_d following Bolton (1980; T_c and T_d in Celsius):

$$e_s = 6.112 \times e^{17.67 \times T_c / (T_c + 243.5)},$$

$$e_a = 6.112 \times e^{17.67 \times T_d / (T_d + 243.5)}.$$

The following empirical formulation from Fosberg (1978) then related RH and T (converted from the original Fahrenheit equations to Celsius) to EMC:

$$\text{EMC} = 0.032\,29 + 0.262\,577 \times \text{RH} - 0.001\,04 \times \text{RH} \times T_c, \\ \text{RH} < 10\%,$$

$$\text{EMC} = 1.754\,40 + 0.160\,107 \times \text{RH} - 0.026\,611 \times T_c, \\ 10\% \leq \text{RH} \leq 50\%,$$

$$\text{EMC} = 21.0606 + 0.005\,565 \times \text{RH}^2 - 0.0063 \times \text{RH} \\ \times T_c - 0.595\,199 \times \text{RH}, \text{RH} > 50\%,$$

with inputs of air temperature in Celsius and relative humidity in percent yielding EMC values in percent.

Our analysis considered the conditions represented at each hour and western U.S. land grid point in the ERA5 dataset during summer (July–September) at night, with nighttime defined as 0500–1200 UTC, following Chiodi et al. (2021). To examine how the frequencies of nocturnal fire-conductive extremes have changed at a given location over the last 40 years (1981–2020), the nighttime-hourly EMC, H_{PBL} , and u_{10} values at each grid point were first ranked by magnitude within the 1981–2000 period and the fire-conductive $p = 0.05$ values (i.e., 95th percentile u_{10} , 95th percentile H_{PBL} , and 5th percentile EMC) were selected to represent fire-conductive extremes in the earlier period. The $p = 0.05$ threshold was also recently used to identify annual trends in global fire-weather extremes by Jain et al. (2022). The early period $p = 0.05$ values were then compared with the distribution of conditions at the same

grid point in a period representing recent conditions (2011–20) to quantify how much more (or less) often thresholds representative of fire-conductive extremes in the earlier period have been reached or surpassed in the recent period. As an example, suppose the 95th-percentile value of hourly nocturnal u_{10} in the earlier period was found to be 2 m s^{-1} at a given location and at that location 2 m s^{-1} ranked as the 90th-percentile hourly nocturnal value in the recent period. This would indicate that the frequency at which near-surface wind speeds met or exceeded 2 m s^{-1} in the recent period has been twice that of the earlier period. In other words, nocturnal conditions quantifiable as unusually windy in the 1980s and 1990s would have doubled in frequency during the 2010s. The same would hold if the 5th-percentile (dry) EMC value from the earlier period was found to rank at the 10th percentile in the more recent period.

Following this set of single-variable analyses, we performed a second set of analyses to determine changes in the frequency at which two variables reached fire-conductive extremes simultaneously (same hour of the same night). In other words, we quantified the change in the frequency of nighttime conditions that were simultaneously dry and windy (EMC and u_{10}), dry with a deep PBL (EMC and H_{PBL}) or windy with a deep PBL (u_{10} and H_{PBL}). In the simultaneous case, we relaxed the threshold percentile to $p = 0.2$ (i.e., 80th-percentile u_{10} and H_{PBL} ; 20th-percentile EMC) so that the probability of simultaneous occurrence in the earlier period would be near the single-variable case ($p = 0.05$) if the variables were distributed independently from one another, in which case we would expect a joint probability of $p = 0.2 \times 0.2 = 0.04$. As in the single-variable case, the observational (ERA5) likelihood of experiencing simultaneous fire-conductive conditions in the earlier period (see Figs. A1–A3 in the appendix for illustration) was then compared to the behavior seen in the recent period to quantify early to recent period changes. For example, if the 20th-percentile value of EMC and 80th-percentile value of u_{10} were found in the earlier period to be 7% and 3 m s^{-1} , respectively, we would first quantify the historical likelihood of finding nocturnal conditions that were simultaneously at or below 7% EMC and at or above 3 m s^{-1} u_{10} at the given land grid point in the earlier period. Then, at the same grid point, we would calculate the likelihood of finding conditions in the recent period that were simultaneously at or below 7% and at or above 3 m s^{-1} and compare the earlier versus recent period likelihoods to determine the change in frequency of simultaneously dry and windy nocturnal conditions.

We start with a look at the baseline distribution of nocturnal EMC, u_{10} , and H_{PBL} in the 1981–2000 period across the western United States, northern Mexico, and southern Canada (North American ERA5-Land grid points west of 95°W and bounded by 25° – 50°N).

3. Results

a. Summer nighttime EMC, u_{10} , and H_{PBL} in the 1980s and 1990s

The 5th-percentile EMC values from the earlier period have magnitudes ranging from 1.6% to 19.5% depending on

¹ Dead fuels moistures in the United States are typically grouped according to the (e -folding) time scale it takes them to respond to changes in EMC and their corresponding thicknesses, with 1-h (<0.25 in. diameter), 10-h (0.25–1 in. diameter), 100-h (1–3 in. diameter), and 1000-h (3–8 in. diameter) categories being typical inputs to fire danger indices and wildfire behavior models.

Dry Summer-Nights in the '80s & '90s

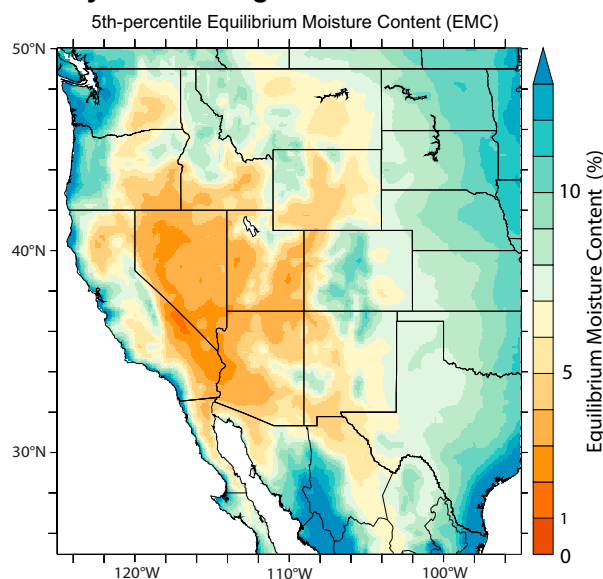


FIG. 1. Low-EMC summer nighttime conditions during the 1981–2000 period. Shading shows the 5th-percentile, hourly, nocturnal EMC value at each land grid cell in the ERA5 dataset. The nighttime hours considered span 0500–1200 UTC July–September.

location, with a median value of 7.7% (Fig. 1). Regions with relatively dry extremes ($<5\%$ EMC) cover the majority of the Great Basin and much of the Colorado River basin. These dry regions include much of Nevada, subregions of Oregon, California, Arizona, Utah, Wyoming, Colorado, and New Mexico, as well as the Snake River Plain in Idaho and the Columbia River basin in Washington. The very driest extremes ($<3\%$ EMC) were seen primarily along the western flanks of the Great Basin, where the study-area minimum occurred in the northern Mojave Desert. Moving west from this minimum, substantially higher values (near or just above 10% EMC) occurred along the western flanks of the southern Sierra Nevada. Thus, large east–west contrasts are evident across Southern California. Relatively high 5th-percentile EMC values ($>10\%$) were found close to the California coast, over western Oregon and Washington and across the Texas Gulf Coast and the northeastern portion of the region depicted in Fig. 1 (North and South Dakota). Similar patterns of moist–dry contrast were apparent in the summertime averages of atmospheric water vapor pressure deficit described by Chiodi et al. (2021). Shared pattern characteristics include dry extremes in the Great Basin and large east–west contrasts across the Sierra Nevada in California and the Cascade Mountains in Washington and Oregon.

The geographic distribution of nocturnal wind speed extremes (u_{10} ; Fig. 2) had a somewhat different pattern than EMC. In the u_{10} case, windier nighttime extremes ($>6 \text{ m s}^{-1}$) are widespread over the Great Plains, whereas lower energy ($2\text{--}4 \text{ m s}^{-1}$) extremes were typical for most of the Rocky Mountain region and terrain to its west. Exceptions include localized energetic ($5\text{--}7 \text{ m s}^{-1}$) extremes in the high plateaus of Washington, Oregon, Idaho, Utah, and Wyoming.

Windy Summer-Nights in the '80s & '90s

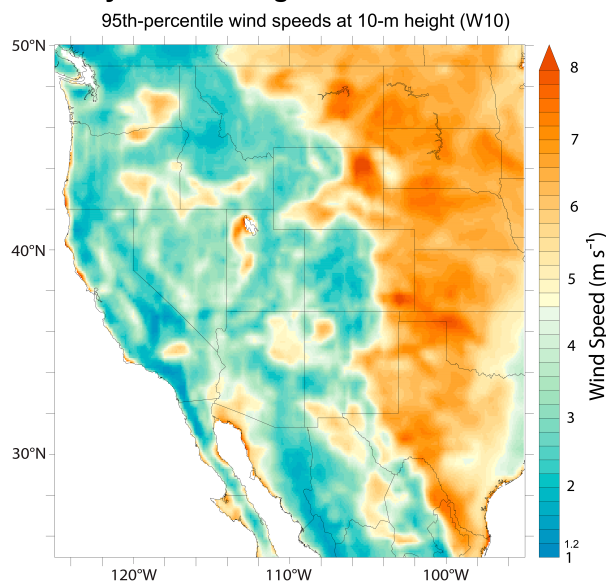


FIG. 2. As in Fig. 1, but for the 95th-percentile nocturnal wind speed u_{10} .

The 95th-percentile H_{PBL} values east of the Rocky Mountains are generally higher than those seen west of the Rocky Mountains (Fig. 3). In this way, the H_{PBL} pattern is similar to that for u_{10} (cf. Figs. 2 and 3). Over the Great Plains, 95th-percentile H_{PBL} values are relatively high ($>700 \text{ m}$), with local maxima in Texas and Montana reaching 900–1000 m. West of the Great Plains, H_{PBL} extremes tended to be substantially lower than 700 m, except over the Great Basin, where localized subregions, mostly in Nevada, have 95th-percentile H_{PBL} values $>1000 \text{ m}$, and portions of the Columbia Plateau in

Deep Boundary Layer, Summer-Nights in the '80s and '90s

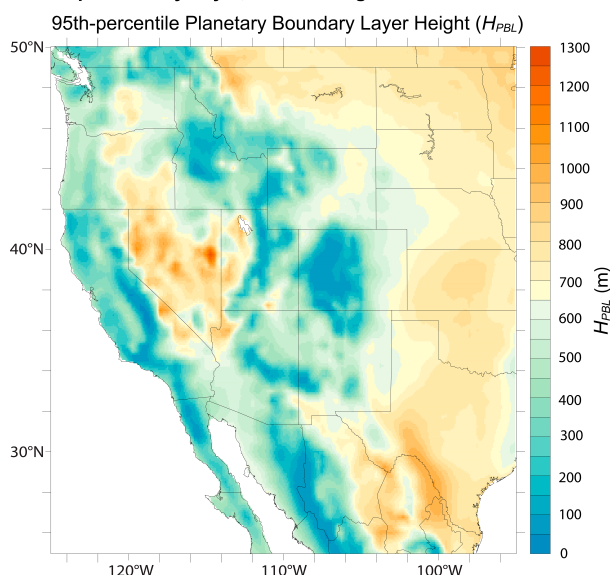


FIG. 3. As in Fig. 1, but for the 95th-percentile PBL height H_{PBL} .

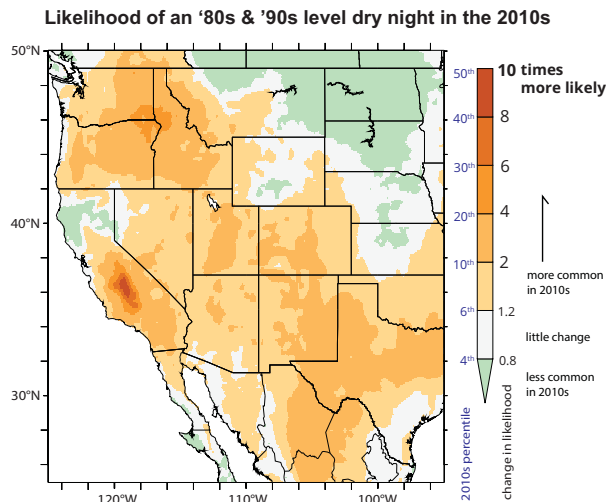


FIG. 4. Recent-period (2011–20) percentile of the earlier period's (1981–2000) 5th-percentile EMC value. Increases (decreases) in the recent compared to earlier percentile indicate that nights with extremely low EMC (dry-fuel nights) have been more (less) frequent in the recent period. For example, a 5th-(earlier) to 10th-(recent) percentile change indicates a doubling in frequency of dry-fuel nights, 5th–20th a quadrupling, etc.

Oregon and Washington, where 95th-percentile H_{PBL} values are similar to those over the Great Plains.

The geographic heterogeneity evident in the distribution of dry-fuel, windy and deep-PBL extremes in the 1981–2000 period (Figs. 1–3) demonstrates that there is a wide range of climatic conditions influencing nocturnal fire behavior across the western United States. We next turn to the salient question of how the rate of occurrence of fire-conducive meteorological extremes has changed at night between the earlier and recent periods.

b. EMC then versus now: 2010s versus 1980s and 1990s

The 5th-percentile EMC analysis results (Fig. 4) illustrate where and by how much the frequency of dry-fuel nights in the recent period has risen compared to the earlier period. Substantial increases in frequency (orange to red hues) are evident over several subregions, including parts of western Idaho, eastern Oregon, and eastern Washington, where dry-fuel nights have become up to $4\times$ more frequent. Over the southern Sierra Nevada and Central Valley in California, dry nights have become even more frequent (up to $10\times$). The rate of dry nighttime extremes has at least doubled over more than a quarter (27%) of the study area, with coherent areas of doubling evident over Texas, New Mexico, Utah, and Colorado. The Great Basin, including the eastern Sierra Nevada, most of New Mexico, southeastern Oregon, and western Utah, was already experiencing some of the driest nocturnal conditions compared to the rest of the western United States in the previous period and has experienced them much more frequently in the recent period (cf. Figs. 1 and 4).

The pattern of EMC change (sign and relative amplitude of change at a given location in Fig. 4) resembles that found previously for VPD (cf. Chiodi et al. 2021), supporting the

expected link between atmospheric demand and fuel moisture. Increases in the frequency of dry-fuel nights were not seen over all regions, however: Decreases occurred over the northeastern part of the study region (eastern Montana, North Dakota, and South Dakota) and parts of Northern California. It bears noting that the minority finding of fewer dry nights in some places, notably over fire-prone portions of Northern California, does not necessarily mean that recent fires in those regions were unaffected by unusually dry conditions at the time of burn. Rather, it means that if they were, then such burn-period dryness would run contrary to the decadal-time scale changes documented here. Nonetheless, that the majority (75%) of the study region experienced increases suggests that these results are consistent with the hypothesis that nighttime fire activity over the western United States has risen, at least in part, due to dryer fuels.

c. Boundary layer depth and wind speed extremes, then versus now

Results from the 95th-percentile H_{PBL} analysis indicate that the frequency of relatively deep nighttime boundary layers has increased over 60% of the study region (Fig. 5a, note the scale bar in Fig. 5 spans a much smaller range than that in Fig. 4). A broad north–south gradient is evident in the results, with increases more prevalent in the south than north. For example, 69% of the terrain north of 42°N has experienced decreases in deep-PBL frequency, whereas deep-PBL conditions have become more frequent over 78% of the area south of 42°N . Northern locations with deep-PBL increases are largely confined to eastern Washington and Oregon. This contrasts with northern-region EMC behavior, in which case the majority of the inland Pacific Northwest exhibited more frequent dry-fuel extremes and a regional maximum spans the Blue Mountains of eastern Washington and Oregon and the western flanks of the Bitterroot Mountains in Idaho. The study-area maximum increase in the frequency of deep-PBL nocturnal conditions is in northeastern New Mexico, where high H_{PBL} extremes have become 2.4 times more frequent in the recent period.

Results of the analysis for changes in the frequency of windy nights (u_{10}) are shown in Fig. 5b. Visual comparison with the deep-PBL results (Fig. 5a) reveals a broad resemblance between the H_{PBL} and u_{10} results (spatial correlation of 0.67), with increasing rates of fire-conducive extremes in both winds and boundary layer depth coinciding over many areas, especially New Mexico and western Texas (cf. Figs. 5a,b). Closer inspection does reveal some localized disparities between the H_{PBL} and u_{10} results, however. Over the northern Sierra Nevada, for example, increases in the frequency of extreme nocturnal wind speeds are evident despite decreases in the frequency of deep-PBL nights. The regional maximum in the u_{10} case also occurs along the flanks of the southern Sierra Nevada where windy nights have been 2.75 times more frequent in the recent period, but H_{PBL} change has been lower in amplitude. Localized differences between u_{10} and H_{PBL} results are also apparent in eastern Washington and Oregon, Wyoming, and Colorado, where the increases in the frequency of windy nights are more spatially coherent than in the H_{PBL} case. Correspondingly, the

Likelihood of an '80s & '90s level deep-PBL or windy night in the 2010s

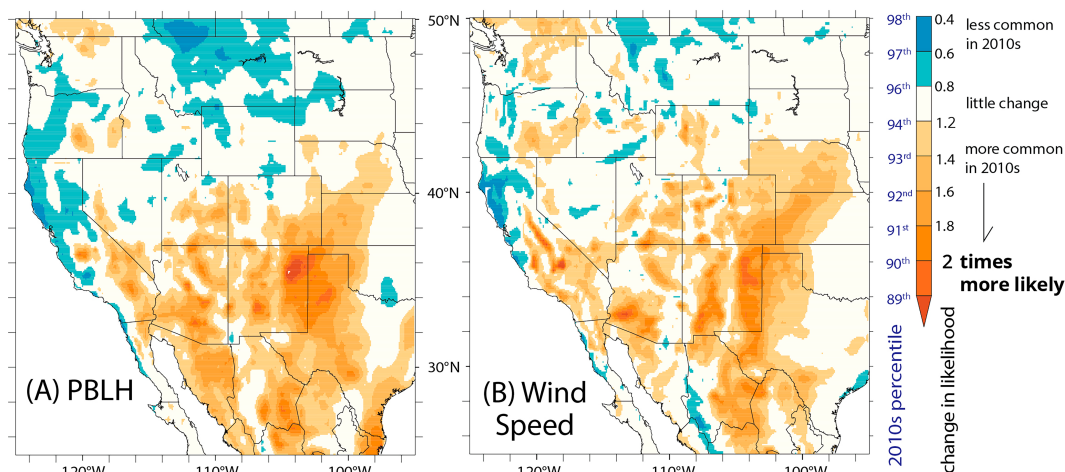


FIG. 5. (a) The recent-period (2011–20) percentile of the 95th-percentile (high extreme) H_{PBL} value from the earlier (1991–2000) period. (b) As in (a), except for u_{10} .

fraction of the northern ($>42^\circ\text{N}$) study region that experienced increases in the frequency of u_{10} extremes (48%) is larger than for H_{PBL} (31%). Spatially coherent increases in u_{10} extremes also occurred over northeastern New Mexico, southeastern Colorado, and western Texas, which were already nocturnally windy compared to the rest of the study area in the previous period (cf. Fig. 2) and have become substantially windier in the recent period (cf. Fig. 5b).

d. Changing frequency of simultaneous fire-conductive meteorological extremes

We next focus our attention on understanding the extent to which there has been a change in the frequency at which fire-conductive conditions have occurred simultaneously (same hour of a given night) in the recent compared to the previous period. Results quantifying such change for the H_{PBL} and u_{10} combination are illustrated in Fig. 6 and show that the frequency of simultaneously windy and deep-PBL conditions has increased over 70% of the study region. As in the single-variable H_{PBL} and u_{10} cases (Figs. 5a,b), increases are more prevalent in the southern part of the study area than in the north. Particularly, the distribution of land north of 42°N is quite evenly split between areas with increased (51%) versus decreased (49%) frequency of fire-conductive H_{PBL} and u_{10} coincidence, whereas 82% of the land south of 42°N experienced an increase in the frequency of simultaneously windy and deep-PBL nocturnal conditions in the recent compared to earlier period. The maximum amplitudes of the changes in the north are also less than in the south, with the largest northern increase of $1.7\times$ over north-central Washington being only about two-thirds as large as the southern region positive maxima of $2.5\times$ over the Sierra Nevada and Colorado. Coherent increases in H_{PBL} and u_{10} simultaneity ranging from factors of 1.25 to $2\times$ are also evident over the southern Great Plains in New Mexico and western Texas.

The frequency of nights with both dry fuels and deep boundary layers has increased over most of the western

United States (Fig. 7a). Spatially coherent areas with at least a doubling in frequency cover much of the interior northwest (e.g., eastern Oregon and eastern Washington; the Snake River Basin and Bitterroot Mountains of Idaho and western Montana), as well as Southern California and the southern Great Plains. Overall, 81% of the study area exhibited increases, with 60% of the terrain north of 42°N and 93% of the terrain south of 42°N experiencing more frequent coincidence of dry-fuel and deep-PBL nocturnal conditions in the recent period. Some areas of decreased frequency are evident; most

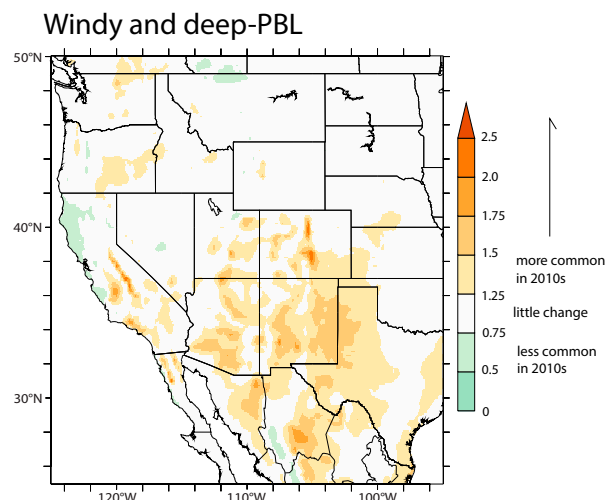


FIG. 6. Ratio of the frequency of simultaneously deeper and windier nocturnal boundary layer conditions in the 2010s compared to the 1980s and 1990s. Ratios greater (less) than 1, denoted by red (green) hues, indicate an increase (decrease) in the frequency of simultaneously windy and deep-PBL nocturnal conditions in the recent (2011–20) compared to the previous (1981–2000) period. Windy and deep-PBL conditions were defined based on 80th-percentile u_{10} and H_{PBL} values, respectively.

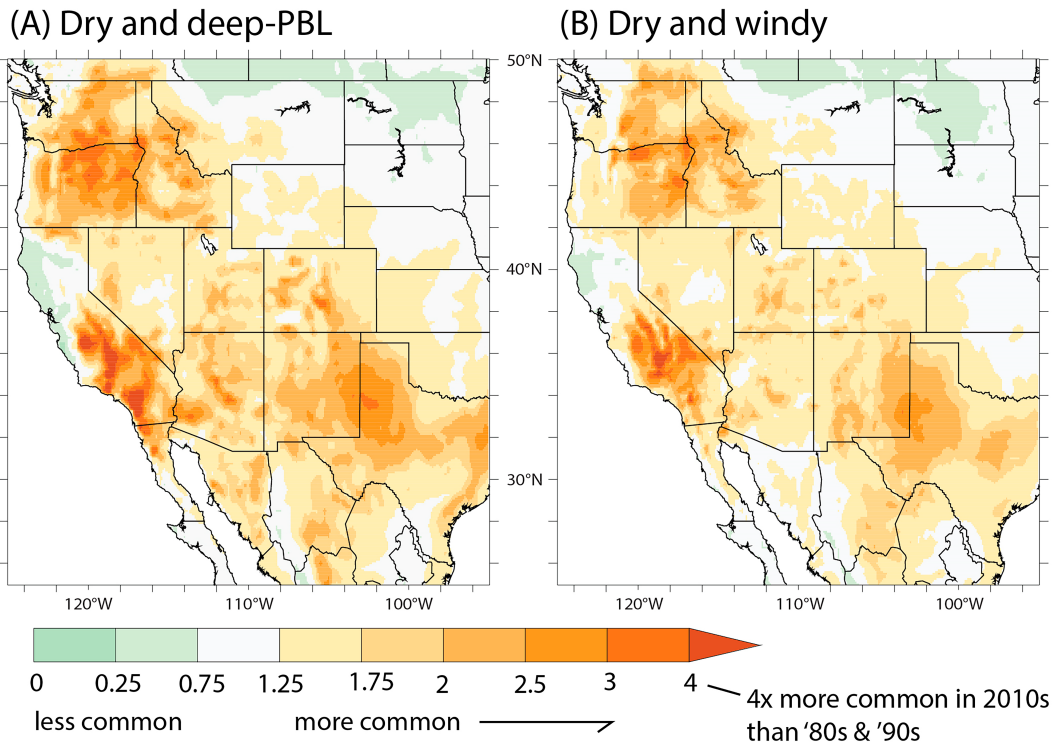


FIG. 7. As in Fig. 6, but for simultaneous (a) EMC and H_{PBL} and (b) EMC and u_{10} fire-conductive extremes.

broadly over the northeastern portion of the study region (north-central Montana; North Dakota; and South Dakota) and, to a lesser extent, over subregions of northern coastal California, which include ecosystems shaped by wildfire (cf. Freeborn et al. 2022). In this respect, California again stands out for its heterogeneity, containing both these decreases along its northern coast and factor 6–8 \times increases over the western flanks of the southern Sierra Nevada, which are surpassed by a peak 12 \times increase along the northwestern foothills of the Tehachapi Mountains.

Results of the simultaneously dry-fuel and windy analysis (Fig. 7b) resemble, in many ways, the dry-fuel and deep-PBL results (Fig. 7a). Relatively large amplitude increases, for example, are evident in both cases over the interior northwest, Southern California, and southern Great Plains. Correspondingly, the spatial correlation between the dry-fuel and deep-PBL and dry-fuel and windy results is strong ($r = 0.86$). This correlation may reflect the dependence of H_{PBL} on vertical wind shear and stem from the drying (increased frequency of low-EMC extremes) being large enough in amplitude and areal extent (cf. Fig. 4) to substantially enhance the overall chance that dry nights coincide with windy or deep-PBL conditions even in the scenario that EMC and u_{10} or H_{PBL} respond mainly to different sources of variability.

Closer inspection reveals some differences between the dry-fuel and windy results compared to dry-fuel and deep-PBL results: The amplitudes of the dry-fuel and deep-PBL increases are often higher than those of the dry-fuel and windy increases in the same region. For example, positive maxima in Southern California reach increases of 7 \times in the dry-fuel and windy case

but are even larger (12 \times) in the dry-fuel and deep-PBL case. Enhancement of dry and deep-PBL increase over dry and windy increase is also evident over the Great Basin.

The fraction of the land grid cells with at least a doubling in frequency of fire-conductive simultaneity is lower for dry and windy (EMC and u_{10} , 11%) conditions than for dry and deep (EMC and H_{PBL} , 27%) conditions. Dry and deep conditions were more abundant especially over the southern Sierra Nevada and interior Pacific Northwest, where deeper boundary layers are, evidently, able to occur without much near-surface wind enhancement. In contrast, H_{PBL} and u_{10} variability appears to be more synchronized over the Great Plains implying that wind shear-driven turbulence (rather than thermodynamic instability) plays a larger role in delaying the formation of stable nocturnal layers in the Great Plains. Despite these differences in detail, however, the frequency of simultaneously dry and deep and dry and windy nocturnal conditions has risen over virtually the same large fraction of the study area (81%).

4. Discussion and conclusions

The results of this study show that dry (low EMC) summer nights have become more frequent over most of the western United States within the career spans of many wildland fire managers. Specifically, 75% of the study domain experienced increases in the rate at which dry-fuel extremes occurred at night in the recent (2011–20) compared to the previous (1981–2000) period. This is based on the definition of nocturnal dry-fuel extremes as 0500–1200 UTC hourly ERA5 equilibrium moisture content at, or below, the previous period's

5th-percentile value at a given location. At least a doubling in the frequency of dry-fuel nights has occurred over 27% of the study region. A quadrupling, or greater, is evident over some wildfire-prone regions, including the interior northwest and Southern California, where maximum increases reach a factor of $12\times$ along the southern coastal mountains and dry-fuel nights have gone from occurring only on occasion (1 in 20) in the 1980s and 1990s to being present 60% of the time in the 2010s.

Changes in western U.S. nocturnal fire meteorology have not been limited to dryness. The frequencies of windy nights and nights with unusually deep planetary boundary layers have also changed within career spans. Over the Northwest, increases in the frequency of deep-PBL nocturnal conditions, defined as hourly nighttime planetary boundary layer height at or above the previous-period 95th percentile, were found in parts of eastern Oregon and Washington. Increases were spread more widely over the southwestern United States and northern Mexico such that 78% of North American ERA5-Land grid points west of 95°W and bounded by 25° – 42°N exhibited more frequent deep-PBL nights, with the largest increase in frequency ($2.4\times$) over northeastern New Mexico. Nearly the same portion (77%) of the Southwest exhibited an increase in the frequency of windy nights with, in this case, the study-region maximum ($2.75\times$) located over the southern Sierra Nevada. Winds and boundary layer depth are known to affect the rate of spread of wildfires and efforts to manage them (e.g., Prichard et al. 2020; USDA Forest Service 2022a,b). The implications of changing nocturnal H_{PBL} and wind conditions for wildfire management therefore deserve further study.

Many western U.S. regions have been subjected to the double (or triple) threat of more nights with simultaneously dry fuels and high winds or deeper boundary layers: Increasing dry-deep and dry-windy simultaneity was found over 81% of the study area. South of 42°N , this fraction rose to 93% and 94%, respectively, with median increases of $1.6\times$ and $1.5\times$. Maximum increases reached a factor of $7\times$ for dry-windy and $12\times$ for dry-deep nights.

Geographically, the western slopes of the Sierra Nevada are a locus for meteorologically driven increase in nocturnal fire susceptibility. This area was already quite dry in terms of EMC in the 1980s and 1990s (Fig. 1), although low compared to some other areas in terms of both H_{PBL} and u_{10} (Figs. 2 and 3). Then, moving to the recent period, it experienced some of the greatest increases in frequencies of low-EMC and large- u_{10} nocturnal conditions (Figs. 4 and 5), along with some of the largest increases in all three of the simultaneous-measure pairings (Figs. 6 and 7).

Increases in the frequency of each of the nocturnal conditions considered herein carry the potential to enhance nocturnal fire behavior. Further study is needed to better understand the role that the changing frequency of simultaneously fire-conductive meteorological extremes (Figs. 6 and 7) has played in changing nocturnal fire behavior. We expect that the results presented herein will help inform this research.

Our motivation for this study was the recognition that nighttime humidity recovery does not occur in isolation and that other simultaneous atmospheric changes (in wind, mixing, and equilibrium fuel moisture) also contribute to fire behavior changes. It is important to understand how each of

these has changed to accurately interpret changes in nighttime fire behavior. Our results show that, indeed, all the atmospheric measures have changed toward supporting more intense nocturnal fire behavior.

These atmospheric properties are themselves dependent on one another. Most obviously, VPD as examined by Chiodi et al. (2021) and EMC are both measures of moisture. Wind speed and boundary layer height are also positively correlated through the contribution of wind shear to boundary layer height. Less directly, or obviously, there is a connection between EMC and H_{PBL} . Drier soils and fuels mean that the soil and fuel surface temperatures increase more rapidly in sunlight and cool more rapidly at night than wet soil and fuels would. Surface temperature drives surface mixing and the (in)stability contribution to boundary layer depth. This suggests that where the results here show H_{PBL} deepening amid drying and decreases (or no change) in wind speed, dryness is increasing the overall nighttime instability owing to the excess heating during the day lasting late enough into the night that it outweighs the later cooling.

These are implications, not direct findings. The intertwined physical processes require direct evaluation if their contributions to nocturnal fire behavior are to be understood. Further investigation of the chain of processes responsible for the relevant nocturnal meteorological changes (cf. Jacobson et al. 2024) and attribution of the observed trends and interannual variability (e.g., Abolafia-Rosenzweig et al. 2022; Holden et al. 2018) will also be necessary to better delineate the predictability of the processes responsible. This is a subject of ongoing group work.

One challenge to statistically evaluating fire-weather linkages at the required subdaily time scale is that the historical records of fire behavior that are generally available over our study period contain information only about fire start dates, severity, and final size (e.g., Eidenshink et al. 2007; Picotte et al. 2020). Successful efforts to better understand the reasons for the typical nocturnal fire behavior (fires laying down at night) and why this behavior has changed (fires lasting longer into the night) will likely require much more detailed (and accurate) records of fire behavior.

Verifiable subdaily records of fire behavior that span our study period, analogous to those developed for the climatological study of other natural phenomena posing threats to life and property (see Knapp et al. 2010, for a century-scale tropical cyclone-based example) may be needed to reach definitive conclusions about the role that meteorological conditions have played in driving the perceived changes in nocturnal fire activity.

Satellite detection of fire activity will undoubtedly play an important role in efforts to produce accurate subdaily fire records (see Liu et al. 2024, for an example spanning 2019–21). Creation, verification, and advancement of such records for both operational products (e.g., Marsha and Larkin 2022; French et al. 2014) and retrospective studies (e.g., Freeborn et al. 2022; Mahood et al. 2022; Giglio et al. 2010) should continue. Pending such development, comparison of the available fire and meteorological records at subdaily time scales to determine which meteorological factors correspond with the greatest changes in nocturnal fire behavior will be fertile ground for future work. Results should be provisionally

evaluated for possible regional climate and ecosystem/vegetation dependencies. Shoulder-season responses should be investigated where the local fire season extends beyond the July–September period considered here. Finally, evaluating the extent to which the observed increases in simultaneously dry, windy, and deep nights are simulated by climate models forced with increasing greenhouse gas concentration will help us understand the extent to which the observed trends should be expected to continue in the coming decades.

Acknowledgments. This work was supported through funding from the U.S. National Fire Plan with additional support for A. M. Chiodi by the Cooperative Institute for Climate, Ocean, and Ecosystem Studies (CICOES) under NOAA Cooperative Agreement NA20OAR4320271, Contribution 2024-1376, and NOAA's Global Ocean Monitoring and Observing (GOMO) Program (<http://data.crossref.org/fundingdata/funder/10.13039/100018302>). This is NOAA PMEL Publication 5951.

Data availability statement. ERA5 data are available at <https://www.ecmwf.int/en/forecasts/datasets/reanalysis-datasets/era5> (accessed 14 October 2022).

APPENDIX

1980s and 1990s Simultaneity

Figures A1–A3 show the probability that nocturnal conditions in the 1981–2000 period were simultaneously windy with a deep PBL (Fig. A1), dry with a deep PBL (Fig. A2), and windy and dry (Fig. A3).

Probability of $H_{\text{pbl}} > 80\text{th}$ & $u_{10} > 80\text{th}$ percentile
1980s and 1990s

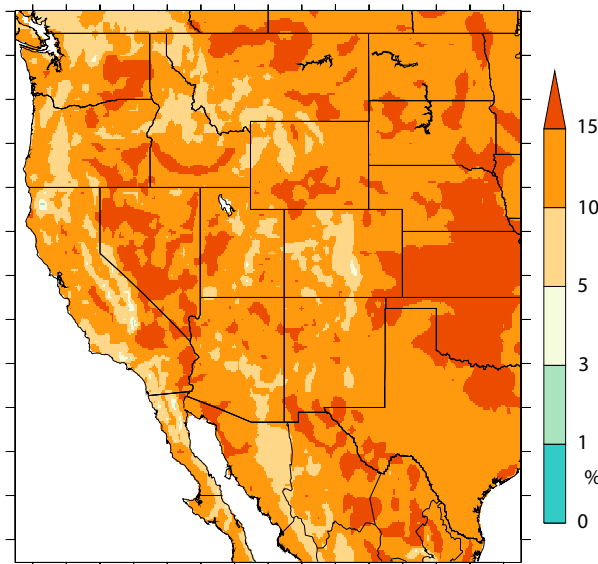


FIG. A1. Probability that H_{PBL} and u_{10} reached fire-conductive levels ($p = 0.2$; deep and windy) at the same hour of the same summer night in the 1981–2000 base period.

Probability of $H_{\text{pbl}} > 80\text{th}$ & $\text{EMC} < 20\text{th}$ percentile
1980s and 1990s

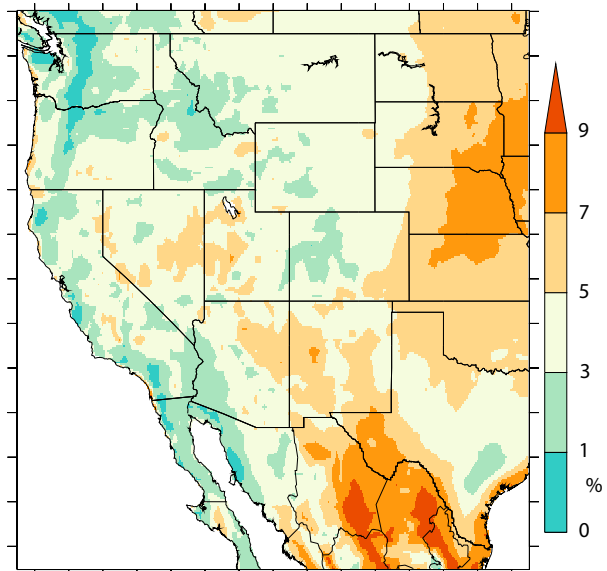


FIG. A2. As in Fig. A1, but for H_{PBL} and EMC (deep and dry).

Probability of $u_{10} > 80\text{th}$ & $\text{EMC} < 20\text{th}$ percentile
1980s and 1990s

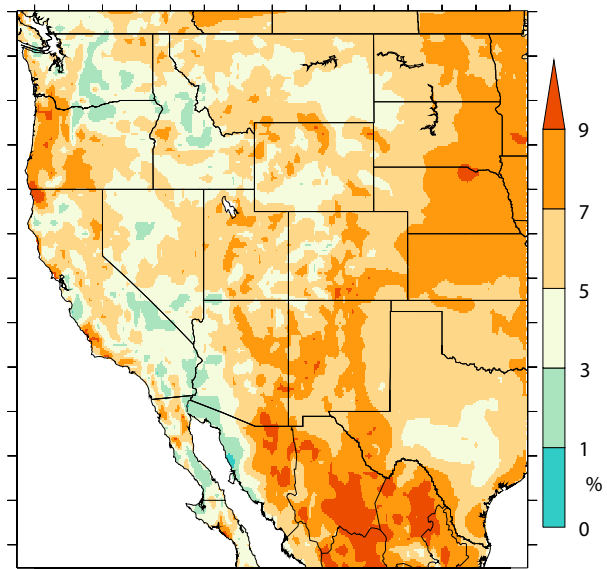


FIG. A3. As in Fig. A1, but for u_{10} and EMC (windy and dry).

REFERENCES

- Abatzoglou, J. T., and A. P. Williams, 2016: Impact of anthropogenic climate change on wildfire across western US forests. *Proc. Natl. Acad. Sci. USA*, **113**, 11 770–11 775, <https://doi.org/10.1073/pnas.1607171113>.
- Abolafia-Rosenzweig, R., C. He, and F. Chen, 2022: Winter and spring climate explains a large portion of interannual variability and trend in western U.S. summer fire burned area.

- Environ. Res. Lett.*, **17**, 054030, <https://doi.org/10.1088/1748-9326/ac6886>.
- Andrews, P. L., C. D. Bevins, and R. C. Seli, 2005: BehavePlus fire modeling system, version 4.0: User's guide. USDA Forest Service General Tech. Rep. RMRS-GTR-106, 132 pp., <https://doi.org/10.2737/RMRS-GTR-106>.
- Archibald, S., C. E. R. Lehmann, J. L. Gómez-dans, and R. A. Bradstock, 2013: Defining pyromes and global syndromes of fire regimes. *Proc. Natl. Acad. Sci. USA*, **110**, 6442–6447, <https://doi.org/10.1073/pnas.1211466110>.
- Balch, J. K., J. T. Abatzoglou, M. B. Joseph, M. J. Koontz, A. L. Mahood, J. McGlinchy, M. E. Cattau, and A. P. Williams, 2022: Warming weakens the night-time barrier to global fire. *Nature*, **602**, 442–448, <https://doi.org/10.1038/s41586-021-04325-1>.
- Bolton, D., 1980: The computation of equivalent potential temperature. *Mon. Wea. Rev.*, **108**, 1046–1053, [https://doi.org/10.1175/1520-0493\(1980\)108<1046:TCOEPT>2.0.CO;2](https://doi.org/10.1175/1520-0493(1980)108<1046:TCOEPT>2.0.CO;2).
- Chiodi, A. M., B. E. Potter, and N. K. Larkin, 2021: Multi-decadal change in western US nighttime vapor pressure deficit. *Geophys. Res. Lett.*, **48**, e2021GL092830, <https://doi.org/10.1029/2021GL092830>.
- Cruz, M. G., M. E. Alexander, P. M. Fernandes, M. Kilinc, and Â. Sil, 2020: Evaluating the 10% wind speed rule of thumb for estimating a wildfire's forward rate of spread against an extensive independent set of observations. *Environ. Modell. Software*, **133**, 104818, <https://doi.org/10.1016/j.envsoft.2020.104818>.
- Eidenshink, J., B. Schwind, K. Brewer, Z.-L. Zhu, B. Quayle, and S. Howard, 2007: A project for Monitoring Trends in Burn Severity. *Fire Ecol.*, **3**, 3–21, <https://doi.org/10.4996/fireecology.0301003>.
- Fosberg, M. A., 1978: Weather in wildland fire management: The fire weather index. *Proc. Conf. on Sierra Nevada Meteorology*, Lake Tahoe, CA, Amer. Meteor. Soc., 1–4, <https://www.frames.gov/catalog/27085>.
- Freeborn, P. H., M. J. Wooster, D. P. Roy, and M. A. Cochrane, 2014: Quantification of MODIS fire radiative power (FRP) measurement uncertainty for use in satellite-based active fire characterization and biomass burning estimation. *Geophys. Res. Lett.*, **41**, 1988–1994, <https://doi.org/10.1002/2013GL059086>.
- , M. W. Jolly, M. A. Cochrane, and G. Roberts, 2022: Large wildfire driven increases in nighttime fire activity observed across CONUS from 2003–2020. *Remote Sens. Environ.*, **268**, 112777, <https://doi.org/10.1016/j.rse.2021.112777>.
- French, N. H. F., and Coauthors, 2014: Modeling regional-scale wildland fire emissions with the Wildland Fire Emissions Information System. *Earth Interact.*, **18**, <https://doi.org/10.1175/EI-D-14-0002.1>.
- Giglio, L., I. Csizsar, and C. O. Justice, 2006: Global distribution and seasonality of active fires as observed with the Terra and Aqua Moderate Resolution Imaging Spectroradiometer (MODIS) sensors. *J. Geophys. Res.*, **111**, G02016, <https://doi.org/10.1029/2005JG000142>.
- , J. T. Randerson, G. R. van der Werf, P. S. Kasibhatla, G. J. Collatz, D. C. Morton, and R. S. DeFries, 2010: Assessing variability and long-term trends in burned area by merging multiple satellite fire products. *Biogeosciences*, **7**, 1171–1186, <https://doi.org/10.5194/bg-7-1171-2010>.
- , W. Schroeder, and C. O. Justice, 2016: The collection 6 MODIS active fire detection algorithm and fire products. *Remote Sens. Environ.*, **178**, 31–41, <https://doi.org/10.1016/j.rse.2016.02.054>.
- Hersbach, H., and Coauthors, 2020: The ERA5 global reanalysis. *Quart. J. Roy. Meteor. Soc.*, **146**, 1999–2049, <https://doi.org/10.1002/qj.3803>.
- Holden, Z. A., and Coauthors, 2018: Decreasing fire season precipitation increased recent western US forest wildfire activity. *Proc. Natl. Acad. Sci. USA*, **115**, E8349–E8357, <https://doi.org/10.1073/pnas.1802316115>.
- Jacobson, T. W. P., R. Seager, A. P. Williams, and N. Henderson, 2022: Climate dynamics preceding summer forest fires in California and the extreme case of 2018. *J. Appl. Meteor. Climatol.*, **61**, 989–1002, <https://doi.org/10.1175/JAMC-D-21-0198.1>.
- , —, I. R. Simpson, K. A. McKinnon, and H. Liu, 2024: An unexpected decline in spring atmospheric humidity in the interior southwestern United States and implications for forest fires. *J. Hydrometeorol.*, **25**, 373–390, <https://doi.org/10.1175/JHM-D-23-0121.1>.
- Jain, P., D. Castellanos-Acuna, S. C. P. Coogan, J. T. Abatzoglou, and M. D. Flannigan, 2022: Observed increases in extreme fire weather driven by atmospheric humidity and temperature. *Nat. Climate Change*, **12**, 63–70, <https://doi.org/10.1038/s41558-021-01224-1>.
- Jolly, W. M., P. H. Freeborn, W. G. Page, and B. W. Butler, 2019: Severe Fire Danger Index: A forecastable metric to inform firefighter and community wildfire risk management. *Fire*, **2**, 47, <https://doi.org/10.3390/fire2030047>.
- , —, L. S. Bradshaw, J. Wallace, and S. Brittain, 2024: Modernizing the US National Fire Danger Rating System (version 4): Simplified fuel models and improved live and dead fuel moisture calculations. *Environ. Modell. Software*, **181**, 106181, <https://doi.org/10.1016/j.envsoft.2024.106181>.
- Knapp, K. R., M. C. Kruk, D. H. Levinson, H. J. Diamond, and C. J. Neumann, 2010: The International Best Track Archive for Climate Stewardship (IBTrACS): Unifying tropical cyclone best track data. *Bull. Amer. Meteor. Soc.*, **91**, 363–376, <https://doi.org/10.1175/2009BAMS2755.1>.
- Little, J. B., 2020: One climate-change wildfire risk lurks in the dark. *Scientific American*, Springer Nature, accessed 19 February 2024, <https://www.scientificamerican.com/article/one-climate-change-wildfire-risk-lurks-in-the-dark/>.
- Liu, T., and Coauthors, 2024: Systematically tracking the hourly progression of large wildfires using GOES satellite observations. *Earth Syst. Sci. Data*, **16**, 1395–1424, <https://doi.org/10.5194/essd-16-1395-2024>.
- Mahood, A. L., E. J. Lindrooth, M. C. Cook, and J. K. Balch, 2022: Country-level fire perimeter datasets (2001–2021). *Sci. Data*, **9**, 458, <https://doi.org/10.1038/s41597-022-01572-3>.
- Marsha, A. L., and N. K. Larkin, 2022: Evaluating satellite fire detection products and an ensemble approach for estimating burned area in the United States. *Fire*, **5**, 147, <https://doi.org/10.3390/fire5050147>.
- Mueller, S. E., A. E. Thode, E. Q. Margolis, L. L. Yocom, J. D. Young, and J. M. Iniguez, 2020: Climate relationships with increasing wildfire in the southwestern US from 1984 to 2015. *For. Ecol. Manage.*, **460**, 117861, <https://doi.org/10.1016/j.foreco.2019.117861>.
- Nelson, R. M., Jr., 2002: An effective wind speed for models of fire spread. *Int. J. Wildland Fire*, **11**, 153–161, <https://doi.org/10.1071/WF02031>.
- Picotte, J. J., K. Bhattarai, D. Howard, J. Lecker, J. Epting, B. Quayle, N. Benson, and K. Nelson, 2020: Changes to the Monitoring Trends in Burn Severity program mapping

- production procedures and data products. *Fire Ecol.*, **16**, <https://doi.org/10.1186/s42408-020-00076-y>.
- Prichard, S. J., N. A. Povak, M. C. Kennedy, and D. W. Peterson, 2020: Fuel treatment effectiveness in the context of landform, vegetation, and large, wind-driven wildfires. *Ecol. Appl.*, **30**, e02104, <https://doi.org/10.1002/eap.2104>.
- Rothermel, R. C., 1972: A mathematical model for predicting fire spread in wildland fuels. USDA Forest Service Research Paper INT-115, 40 pp., <https://research.fs.usda.gov/treesearch/32533>.
- Seager, R., A. Hooks, A. P. Williams, B. Cook, J. Nakamura, and N. Henderson, 2015: Climatology, variability, and trends in the U.S. vapor pressure deficit, an important fire-related meteorological quantity. *J. Appl. Meteor. Climatol.*, **54**, 1121–1141, <https://doi.org/10.1175/JAMC-D-14-0321.1>.
- Seidel, D. J., Y. Zhang, A. Beljaars, J.-C. Golaz, A. R. Jacobson, and B. Medeiros, 2012: Climatology of the planetary boundary layer over the continental United States and Europe. *J. Geophys. Res.*, **117**, D17106, <https://doi.org/10.1029/2012JD018143>.
- Stull, R. B., 1988: *An Introduction to Boundary Layer Meteorology*, Kluwer Academic, 670 pp.
- USDA Forest Service, 2022a: Gallinas-Las Dispensas Prescribed Fire Declared Wildfire Review. USDA Forest Service, 85 pp., <https://www.fs.usda.gov/sites/default/files/gallinas-las-dispensas-prescribed-fire-declared-wildfire-review.pdf>.
- , 2022b: National Prescribed Fire Program Review. USDA Forest Service, 107 pp., <https://www.frames.gov/catalog/66622#:~:text=EXECUTIVE%20SUMMARY%3A%20In%20the%20spring,program%20pending%20a%20program%20review>.
- Weise, D. R., F. M. Fujioka, and R. M. Nelson Jr., 2005: A comparison of three models of 1-h time lag fuel moisture in Hawaii. *Agric. For. Meteorol.*, **133**, 28–39, <https://doi.org/10.1016/j.agrformet.2005.03.012>.
- Williams, A. P., and Coauthors, 2014: Causes and implications of extreme atmospheric moisture demand during the record-breaking 2011 wildfire season in the southwestern United States. *J. Appl. Meteor. Climatol.*, **53**, 2671–2684, <https://doi.org/10.1175/JAMC-D-14-0053.1>.
- , J. T. Abatzoglou, A. Gershunov, J. Guzman-Morales, D. A. Bishop, J. K. Balch, and D. P. Lettenmaier, 2019: Observed impacts of anthropogenic climate change on wildfire in California. *Earth's Future*, **7**, 892–910, <https://doi.org/10.1029/2019EF001210>.